Magnetostatic Wave Propagation in YIG Double Layers

Kunquan Sun and Carmine Vittoria, *Senior Member, IEEE*

Abstract—**This paper presents calculations for the magnetostatic surface wave propagation characteristics in single-crystal double layers of yttrium iron garnet (YIG) with arbitrary direction of magnetization. The induced uniaxial magnetic anisotropy field is assumed to be different in the two layers; hence, the magnetization in one layer is aligned at an angle with respect to the magnetization direction in the other layer. The magnetostatic field interactions between layers depend on the angle between the two magnetization directions and on the separation between the two YIG layers. The wave propagation directions and time delays in each layer can be strongly affected by the application of an applied magnetic field and the magnetostatic coupling between the two layers, as well as by the uniaxial anisotropy energy in each layer.**

I. Introduction

OWING to the successful development of techniques for producing magnetic multilayer films, there has recently been considerable interest in the microwave properties of magnetic multilayer structures. In particular, the study of double-layer systems has been the subject of several investigations [1]–[11], since it is the first step toward the fabrication of multilayers and/or magnetic superlattices. One decade after Damon and Eshbach [12] described the magnetostatic modes in a planar structure, Wolfram [1] gave the first description of magnetostatic waves on double layers. Ganguly and Vittoria [2] examined magnetostatic wave propagation in parallel layers of magnetic materials separated by a dielectric layer. Adkins and Glass [3] and Daniel and Emtage [4] performed measurements of magnetostatic wave propgation in double layers. Zubkov and Epanechnikov [5] indicated that dispersion of surface waves is anomalous when dissimilar layers are in contact, showing regions of negative group velocity. In all of these studies [1]–[11], it has been assumed that the magnetization of each individual layer in double-layer structures is either parallel or antiparallel. In this paper we consider the effect of noncollinear magnetization direction on magnetostatic surface wave propagation in a two-layer magnetic system. We assume that the magnetization in a given magnetic layer is aligned in an arbitrary direction with respect to the magnetization direction in the other layer of a two-layer structure. It has recently been determined experimentally [13] that when the applied magnetic field is small, the magnetizations in each layer of a single-crystal double-layer YIG structure are not parallel to each other because the induced in-plane anisotropy field, H_u, is different in each layer. H_u has been found [13] to be different in each layer, since the strain arising from the substrate strain is different in each layer.

This work is to study the propagation characteristics of magnetostatic waves in a single-crystal structure of GGG/YIG/GGG/YIG, where GGG is the abbreviation for gadolinium gallium garnet. The magnetization orientations in the two YIG films are not collinear when the applied field is small. General formulations of the dispersion relations and time delays are calculated for both YIG films with cubic and induced in-plane anisotropy fields in Section II. Calculated results for the dispersion relations and time delays as a function of magnetic field and separation of the two YIG layers as well as of the uniaxial anisotropy energy in each layer are illustrated in Section III. In Section IV, conclusions are drawn.

Manuscript received May 23, 1989; revised September 17, 1990. This work was supported in part by the ONR.

K. Sun was with the Department of Electrical and Computer Engineering, Northeastern University, Boston, MA. He is now with the Department of Electrical Engineering, Jackson State University, Jackson, MS 39217.

C. Vittoria is with the Department of Electrical and Computer Engineering, Northeastern University, Boston, MA 02115.

IEEE Log Number 9041087.

II. Theory

The geometry of the two-layer structure is shown in Fig. 1, where a paramagnetic GGG film of thickness d_2 is placed between two YIG films, and the GGG substrate is assumed to be infinitely thick. In Fig. 2, the two magnetizations of the two YIG layers are represented by $\vec{M}_1$ and $\vec{M}_2$, respectively. Angular orientations of $\vec{M}_1$ and $\vec{M}_2$ are also shown in Fig. 2, where the capital letters, X_c, Y_c, and Z_c, refer to the crystal axes while (ϕ, β), (ϕ_1, θ_1), and (ϕ_2, θ_2) refer to the angular distributions of $\vec{H}_a$, $\vec{M}_1$, and $\vec{M}_2$, respectively.

In order to maximize the effect of substrate lattice mismatch on the direction of $\vec{M}$ in the film plane, we choose the film plane to be a {110} plane. With no strain one would expect $\vec{M}$ to be parallel to the $\langle 111 \rangle$ axis in both films. But if there are strains induced by lattice mismatch between substrate and film, a uniaxial anistropy field is induced in the film. The effect of this field is to "push" $\vec{M}$ away from the $\langle 111 \rangle$ axis. Hence, we will have realized a situation in which the magnetizations are not necessarily parallel to each other in the two films if the films are strained independently. Films of the {100} type do not induce any uniaxial field in the film plane even if the films are strained.

An external static magnetic field, $\vec{H}_a$, is applied in the film plane so that the internal fields $\vec{H}_0^{(1)}$ and $\vec{H}_0^{(2)}$ also lie in the planes of the two YIG layers. The quantities $\vec{H}_0^{(1)}$ and $\vec{H}_0^{(2)}$ can be expressed [14] in terms of the external field $\vec{H}_a$, the static cubic anisotropy field components $\vec{H}_A^{(1)}$ and $\vec{H}_A^{(2)}$, and the static induced in-plane anisotropy field components $\vec{H}_u^{(1)}$ and $\vec{H}_u^{(2)}$, where the superscripts (1) and (2) denote the

0018-9480/91/0200-0339$01.00 ©1991 IEEE

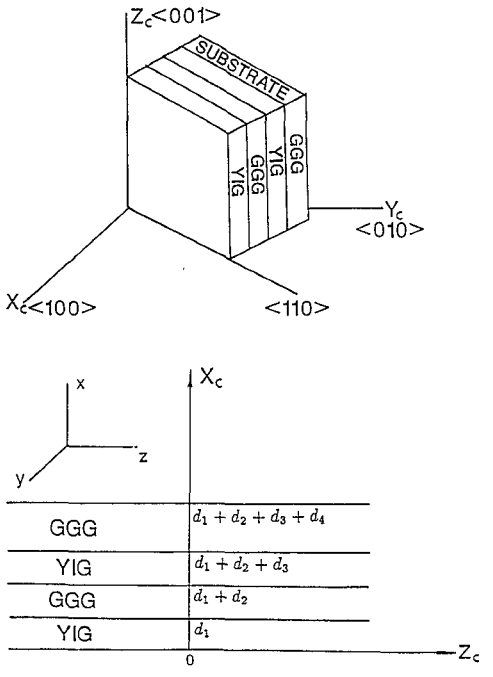

Fig. 1. A cross view of the geometrical configuration of the double-layer YIG film.

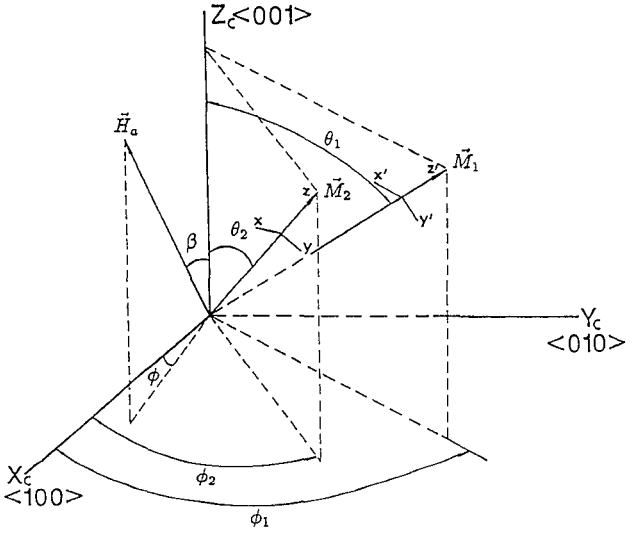

Fig. 2. The three coordinate systems of interest. The capital letters, X_c, Y_c, and Z_c, refer to the crystal axes. (x, y, z) and (x', y', z') refer to layer 2 ($\vec{M}_2$) and layer 1 ($\vec{M}_1$); z and z' are parallel to $\vec{M}_2$ and $\vec{M}_1$, respectively.

layers corresponding to $\vec{M}_1$ and $\vec{M}_2$. Mathematical expressions for $\vec{H}_0^{(1)}$ and $\vec{H}_0^{(2)}$ are given below:

$$\vec{H}_0^{(i)} = \vec{H}_a - 2K_1^{(i)}\Big[\left(\alpha_2^{(i)^2} + \alpha_3^{(i)^2}\right)\alpha_1^{(i)}\hat{a}_X + \left(\alpha_1^{(i)^2} + \alpha_3^{(i)^2}\right)\alpha_2^{(i)}\hat{a}_Y + \left(\alpha_1^{(i)^2} + \alpha_2^{(i)^2}\right)\alpha_3^{(i)}\hat{a}_Z\Big]/M_i + \frac{2K_u^{(i)}}{M_i}\alpha_3^{(i)}\hat{a}_Z, \qquad i = 1,2 \tag{1a}$$

or

$$\vec{H}_0^{(i)} = \vec{H}_a + \vec{H}_A^{(i)} + \vec{H}_u^{(i)}, \qquad i = 1,2 \tag{1b}$$

where $K_1^{(i)}$ and $K_u^{(i)}$ are the cubic magnetocrystalline and uniaxial anistropy energy constants, respectively, the $\alpha^{(i)}$'s are the direction cosines of $\vec{M}_i$ $(i = 1,2)$ with respect to the cubic axes, and $\hat{a}_X$, $\hat{a}_Y$, and $\hat{a}_Z$ are the unit vectors in crystal coordinates (see Fig. 2). The static demagnetizing field is zero for $\vec{H}_a$ in the plane of the YIG films. It is noted that the uniaxial axis is along the [001] or the Z_c axis. Since $K_u > 0$, the easy axis of magnetization is along the [001] axis.

As in previous theoretical developments [14], the magnetostatic dispersion relations may be expressed in terms of permeability tensor elements for each magnetic layer. We start with the well-known Landau–Lifshitz equation of motion with no damping and adapt previous formulations [14] to the case of the applied field in the $(1\bar{1}0)$ plane. After some algebraic manipulations, the permeability tensors corresponding to $\vec{H}_a$ applied in the film plane $(i = 1,2)$ are obtained:

$$\mu^{(i)} = \begin{pmatrix} u_{11}^{(i)} & -i\mu_{12}^{(i)} & 0 \\ i\mu_{12}^{(i)} & \mu_{22}^{(i)} & 0 \\ 0 & 0 & 1 \end{pmatrix} \tag{2}$$

where

$$\mu_{11}^{(i)} = 1 - \frac{\Omega_{y_i}}{\Omega_i^2 - \Omega_{H_i}^2}$$

$$\mu_{22}^{(i)} = 1 - \frac{\Omega_{x_i}}{\Omega_i^2 - \Omega_{H_i}^2}$$

$$\mu_{12}^{(i)} = \frac{\Omega_i}{\Omega_i^2 - \Omega_{H_i}^2}$$

$$\Omega_{x_i} = \left(H_0^{(i)} - M_i a_i\right)/4\pi M_i$$

$$\Omega_{y_i} = \left(H_0^{(i)} - M_i b_i\right)/4\pi M_i$$

$$\Omega_i = \frac{\omega}{|\gamma|}\frac{1}{4\pi M_i}$$

$$\Omega_{H_i}^2 = \Omega_{x_i}\Omega_{y_i}$$

$$a_i = 2K_1^{(i)}\left(1.5\sin^2\theta_i - 1\right)/M_i^2$$

$$b_i = 2K_1^{(i)}\left(1.125\sin^2\theta_i - 1\right)/M_i^2 - 2K_u^{(i)}\sin\theta_i/M_i^2$$

and $i = 1,2$ denotes the coordinate systems (x', y', z') and (x, y, z) associated with the magnetizations $\vec{M}_1$ and $\vec{M}_2$, respectively. The coefficients a_i and b_i have been derived previously [14]. By solving the equilibrium condition equations based on minimizing the free energy of each magnetic layer, it is found [13] that the equilibrium azimuthal angles of $\vec{M}_1$ and $\vec{M}_2$ are equal to 45°, or $\phi_1 = \phi_2 = 45°$, since $\vec{H}_a$ is in the film plane. This implies that both $\vec{M}_1$ and $\vec{M}_2$ lie in the $\{1\bar{1}0\}$ plane, which is also the film plane. The polar angles θ_1 and θ_2 are not equal if the applied magnetic field is low compared with the magnetic anisotropy fields, $H_u^{(1)}$ and $H_u^{(2)}$. The angular parameters (ϕ_1, θ_1) and (ϕ_2, θ_2) at equilibrium are substituted into (2) in order to determine the permeabilities $\mu^{(1)}$ and $\mu^{(2)}$.

We introduce two coordinate systems, since there are two magnetic layers to consider. The primed system (x', y', z') corresponds to layer 1 ($\vec{M}_1$) and the unprimed (x, y, z) to layer 2 ($\vec{M}_2$). We choose z' and z to be parallel to the static

magnetization directions $\vec{M}_1$ and $\vec{M}_2$, respectively (see Fig. 2). Both y' and y lie in the film plane but x' and x are directed normal to the film plane. The angle between y' and y or z' and z is equal to $\theta_1 - \theta_2 = \alpha$ and is a measure of misalignment between the two magnetization directions. We will examine the magnetostatic wave propagation in the (x, y, z) system as shown in Fig. 2. The "free" surface of one YIG layer is located at $x = 0$. In the following calculations, $\vec{M}_1$ is in the $\langle 111 \rangle$ direction and $\vec{M}_2$ is α degrees away relative to $\vec{M}_1$, and the uniaxial field of layer 2 is in the $\langle 100 \rangle$ direction.

Under the magnetostatic approximation $\vec{h}_m = -\nabla\psi$, where ψ is a magnetic scalar potential, combined with $\vec{B} = \mu_0 \mu \cdot \vec{h}_m$, we have

$$\frac{\partial^2\psi}{\partial x^2} + \frac{\partial^2\psi}{\partial y^2} + \frac{\partial^2\psi}{\partial z^2} = 0, \qquad -\infty < z \leqslant 0 \tag{3}$$

$$\mu_{11}^{(2)}\frac{\partial^2\psi}{\partial x^2} + \mu_{22}^{(2)}\frac{\partial^2\psi}{\partial y^2} + \frac{\partial^2\psi}{\partial z^2} = 0, \qquad 0 < x \leqslant d_1 \tag{4}$$

$$\frac{\partial^2\psi}{\partial x^2} + \frac{\partial^2\psi}{\partial y^2} + \frac{\partial^2\psi}{\partial z^2} = 0, \qquad d_1 < x \leqslant d_1 + d_2 \tag{5}$$

$$\mu_{11}^{(1)}\frac{\partial^2\psi}{\partial x'^2} + \mu_{22}^{(1)}\frac{\partial^2\psi}{\partial y'^2} + \frac{\partial^2\psi}{\partial z'^2} = 0,$$

$$d_1 + d_2 < x \leqslant d_1 + d_2 + d_3 \tag{6}$$

$$\frac{\partial^2\psi}{\partial x^2} + \frac{\partial^2\psi}{\partial y^2} + \frac{\partial^2\psi}{\partial z^2} = 0, \qquad d_1 + d_2 + d_3 < x < \infty. \tag{7}$$

The requirement that ψ vanish at $x = \pm\infty$ yields

$$\Psi_I(x, y, z) = C_1 e^{kx - jk_y y - jk_z z}, \qquad -\infty < x \leqslant 0 \tag{8}$$

$$\Psi_{II}(x, y, z) = \left(C_2 e^{\kappa x} + C_3 e^{-\kappa x}\right) e^{-jk_y y - jk_z z}, \qquad 0 < x \leqslant d_1 \tag{9}$$

$$\Psi_{III}(x, y, z) = \left(C_4 e^{kx} + C_5 e^{-kx}\right) e^{-jk_y y - jk_z z}, \qquad d_1 < x \leqslant d_1 + d_2 \tag{10}$$

$$\Psi_{IV}(x', y', z') = \left(C_6 e^{\kappa' x'} + C_7 e^{-\kappa' x'}\right) e^{-jk_y' y' - jk_z' z'}, \qquad d_1 + d_2 < x \leqslant d_1 + d_1 + d_2 + d_3 \tag{11}$$

$$\Psi_V(x, y, z) = C_8 e^{-kx - jk_y y - jk_z z}, \qquad d_1 + d_2 + d_3 < x < \infty \tag{12}$$

where (κ, k_y, k_z) and (κ', k_y', k_z') are the wavenumbers corresponding to the (x, y, z) and (x', y', z') coordinate systems, respectively, and

$$k^2 = k_y^2 + k_z^2 \tag{13}$$

$$\kappa^2 = \frac{\mu_{22}}{\mu_{11}}k_y^2 + \frac{1}{\mu_{11}}k_z^2 \qquad \left(\mu_{11} = \mu_{11}^{(2)}, \mu_{22} = \mu_{22}^{(2)}\right) \tag{14}$$

$$\kappa'^2 = \frac{\mu_{22}^{(1)}}{\mu_{11}^{(1)}}\left(k_y^2\cos^2\alpha - k_y k_z \sin 2\alpha + k_z^2 \sin^2\alpha\right) + \frac{1}{\mu_{11}^{(1)}}\left(k_y^2 \sin^2\alpha + k_y k_z \sin 2\alpha + k_z^2\cos^2\alpha\right). \tag{15}$$

We use transformation matrix $[T]$ in deriving (15) and (16), where

$$[T] = \begin{pmatrix} 1 & 0 & 0 \\ 0 & \cos\alpha & -\sin\alpha \\ 0 & \sin\alpha & \cos\alpha \end{pmatrix}.$$

By using the boundary conditions whereby the tangential components of $\vec{h}_m$ and the normal components of $\vec{B}$ are continuous, the following transcendental equation is obtained:

$$\left(P^{(1)}Q^{(1)}e^{-2\kappa' d_3} - 1\right)\left(1 - P^{(2)}Q^{(2)}e^{-2\kappa d_1}\right) + P^{(1)}Q^{(2)}e^{-2kd_2}\left(1 - e^{-2\kappa d_1}\right)\left(1 - e^{-2\kappa' d_3}\right) = 0 \tag{16}$$

where

$$P^{(1)} = \frac{1 - p^{(1)}}{1 + p^{(1)}}$$

$$Q^{(1)} = \frac{1 - q^{(1)}}{1 + q^{(1)}}$$

$$P^{(2)} = \frac{1 - p^{(2)}}{1 + p^{(2)}}$$

$$Q^{(2)} = \frac{1 - q^{(2)}}{1 + q^{(2)}}$$

$$p^{(1)} = \frac{\kappa'}{k}\mu_{11}^{(1)} + \left(\frac{k_y}{k}\cos\alpha - \frac{k_z}{k}\sin\alpha\right)\mu_{12}^{(1)}$$

$$q^{(1)} = \frac{\kappa'}{k}\mu_{11}^{(1)} - \left(\frac{k_y}{k}\cos\alpha - \frac{k_z}{k}\sin\alpha\right)\mu_{12}^{(1)}$$

$$p^{(2)} = \frac{\kappa}{k}\mu_{11} + \frac{k_y}{k}\mu_{12}$$

$$q^{(2)} = \frac{\kappa}{k}\mu_{11} - \frac{k_y}{k}\mu_{12}.$$

We wish now to discuss the relevance of (16). This equation includes two terms. The first term is recognized as the dispersion of two individual magnetic layers which are not magnetically and electromagnetically coupled, and the second includes the effect of the coupling between the two magnetic layers. For example, if the separation d_2 between the two YIG layers is set to infinity, the coupling term vanishes from (16). Then, only two dispersion relations are obtained, corresponding to the two layers. This means that magnetostatic surface waves propagate in the two layers without affecting each other. In this limit ($d_2 \to \infty$) the angle α has no effect on the dispersion. Other limiting cases to consider are the following.

1) $\vec{M}_1 = \vec{M}_2$: Equation (16) results in a dispersion relation which is consistent with that given in [6] and [8].
2) In the limit of either $d_2 = \infty$ or $d_2 = 0$, $\vec{M}_1 = \vec{M}_2$, (16) reduces to the dispersion equation for a single layer derived by Damon and Eshbach [12].

Let us now examine the general case in which d_1, d_2, and d_3 are finite. Our greatest interest is usually in propagation perpendicular to the magnetization, when the bandwidth is greatest [12]. When the films are far apart we expect two surface wave bands whose greatest widths are at an angle α to each other, α being the angle between the magnetizations. When the films are brought closer their properties become

collective, and it is necessary to explore the three-dimensional dispersion function $\omega(k_y, k_z)$ to find where the frequency in each band is highest. These directions are not necessarily the directions of greatest bandwidth, because regions of negative group velocity exist [2], [5].

III. Results and Discussion

Based on the dispersion equation (16), a three-dimensional plot (ω versus k_y and k_z) is obtained (see Fig. 3a) where there exist the two branches. The assumed parameters for one layer are $4\pi M = 1750$ G, $2K_1/M = -82$ Oe, $2K_u/M = 0$, and $d_1 = 1$ μm; for the other layer $4\pi M = 1256$ G, $2K_1/M = -82$ Oe, $2K_u/M = 50$ Oe, and $d_3 = 1$ μm. The separation between the two magnetic layers is $d_2 = 1$ μm. The top branch corresponds to layer 1 while the bottom branch corresponds to layer 2. Because of the different static magnetizations and induced in-plane anisotropy fields H_u in the two different layers and the coupling between the two layers, the dispersion for layer 1 differs from that of layer 2. One feature of the bottom branch is that there exists a cutoff frequency region. The other feature is the existence of an anomalous region where $d\omega/dk < 0$ [2], [5].

The intersection of the ω = constant plane and the surface contour of the $\omega(k_y, k_z)$ dispersion determines the allowable values of k_y and k_z in the layered medium. For example, for $\omega = 1$ GHz, we show in Fig. 3(b) the locus of points at the intersection of $\omega = 1$ GHz with the dispersion surface in the $y-z$ plane. The magnetostatic wave at a fixed frequency will have different velocities if it propagates in different directions in the $y-z$ plane. This is because, for a given frequency, the wavenumber $k = \sqrt{k_y^2 + k_z^2}$ takes on different values depending on the set of values for k_y and k_z. Similarly, for $\omega = 0.8052$ GHz, we have another intersection curve, shown in Fig. 3(c), which is different from that in Fig. 3(b). In Fig. 3(b), the magnetostatic wave can propagate in any direction (θ_k varying from 0 to 90°), while in Fig. 3(c), the magnetostatic wave can only propagate over a narrow angular range.

In order to understand the three-dimensional dispersion, we examine the dispersion by varying k with fixed azimuthal angle θ_k. Parts (a), (b), and (c) of Fig. 4 illustrate the dispersions with $\theta_k = 0$, 45°, and 90°, respectively, where the applied magnetic field is set to $H = 0$, the separation between the two layers $d_2 = 1$ μm, and $\alpha = 24°$. Fig. 4(a) gives the dispersions of two individual magnetic layers without any magnetic coupling as well as the dispersions with the magnetic coupling taken into account in (16). Owing to the magnetostatic interaction (see Fig. 4(a)), the two branches repel each other over the wide range of k ($10^2 \sim 10^4$). When the propagation direction is rotated from $\theta_k = 0$ to $\theta_k = 45°$, the two branches are active at lower frequencies but the splitting is not sensitive to the change of k. By increasing θ_k to 90°, there exists only one branch, which allows magnetostatic wave propagation in layer 1 but not in layer 2. For the rest of this paper, we will focus on ω versus k_y and k_z regions in which propagation is allowable in both layers.

Fig. 5 shows the time delays corresponding to the dispersions for $\theta_k = 0$. It is obvious that for a given frequency, the delay times associated with magnetostatic waves which are coupled show greater delays than those waves without coupling. We find that in layer 2 there exists a peak in time delay at $f_0 = 0.7$ GHz.

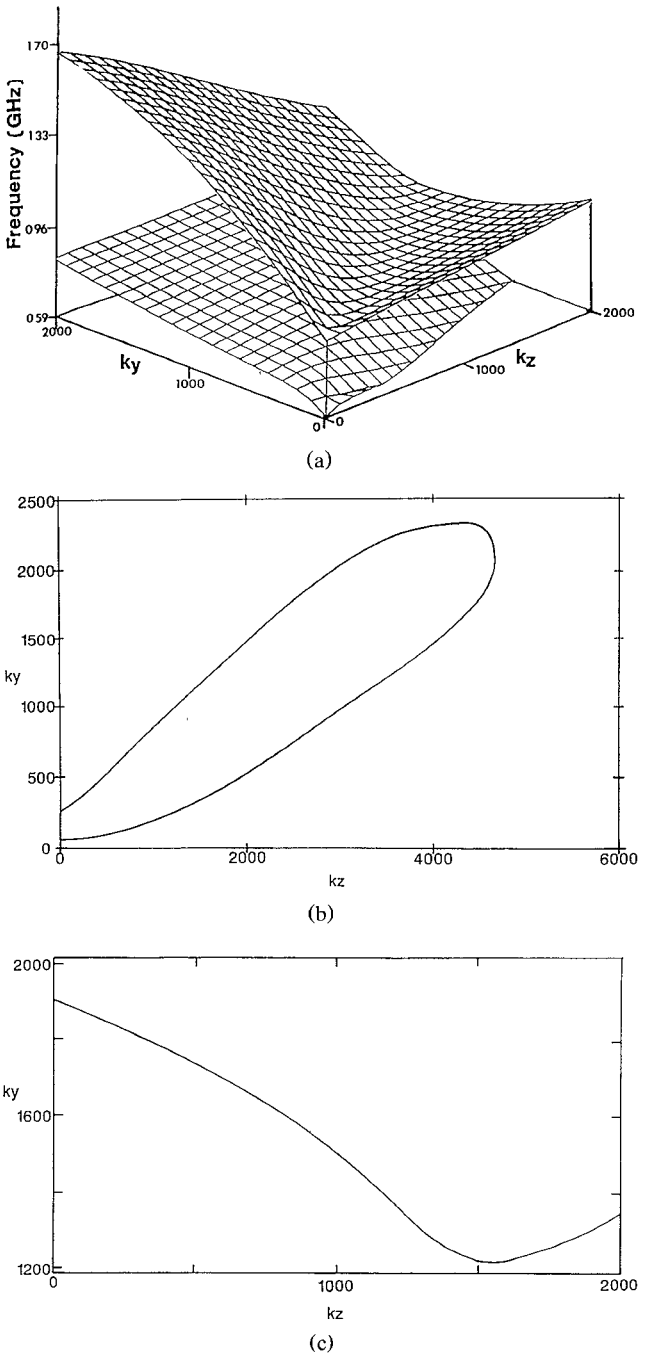

Fig 3. (a) Three-dimensional dispersion (ω, k_y, k_z). $H = 0$, $\alpha = 24°$, and $d_2 = 1$ μm. (b) The intersection of the $\omega = 1$ GHz plane and the surface contour of $\omega(k_y, k_z)$ from Fig. 3(a). (c) The intersection of the $\omega = 0.8052$ GHz plane and the surface contour of $\omega(k_y, k_z)$ from Fig. 3(a).

The effect of the separation between the two magnetic layers on the dispersions and time delays of the two-layer system is demonstrated in Figs. 6 and 7, where the separation d_2 is varied from 0.1 μm to 10 μm and the other parameters are assumed to be the same as before. As the separation between the two magnetic layers increases, the splitting between the two branches of the dispersion decreases while the time delay difference in each layer

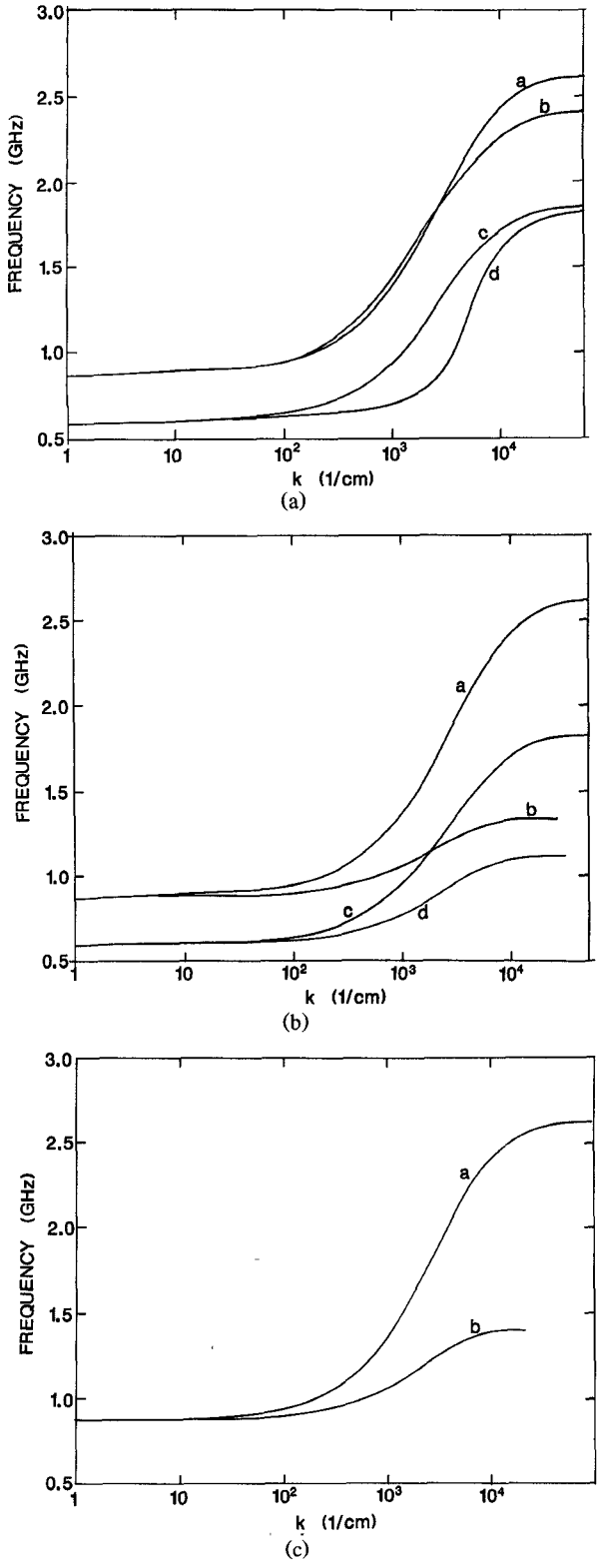

Fig. 4. (a) Dispersion with $\theta_k = 0$, $H = 0$, and $\alpha = 24°$.

a: Dispersion for layer 1 without coupling ($d_2 \to \infty$).
b: The branch corresponding to layer 1 with coupling. k lies in $y-z$ plane and is normal to $\vec{M}_1$.
c: Dispersion for layer 2 without coupling ($d_2 \to \infty$).
d: The branch corresponding to layer 2 with coupling. k lies in $y-z$ plane and is normal to $\vec{M}_2$.

(b) The notation is the same as that of Fig. 4(a) except for $\theta_k = 45°$.
(c) Dispersion with $\theta_k = 90°$, $H = 0$, and $\alpha = 24°$:

a: Dispersion for layer 1 without coupling ($d_2 \to \infty$).
b: The branch corresponding to layer 1 with coupling.

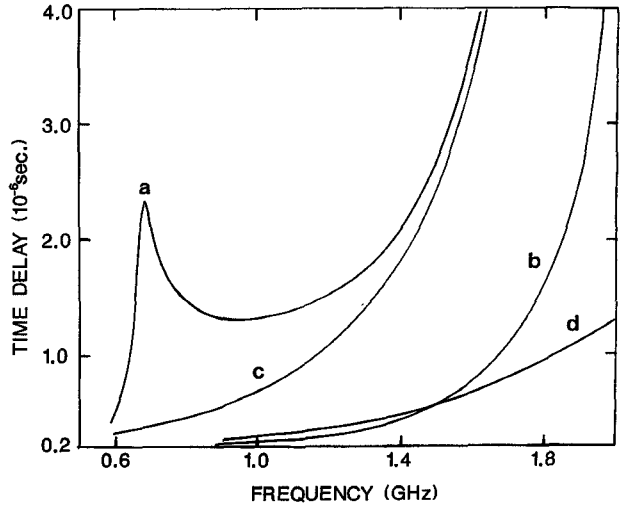

Fig. 5. Time delay versus frequency. $\theta_k = 0$, $H = 0$, and $\alpha = 24°$.

a: Corresponds to layer 2 with coupling.
b: Corresponds to layer 1 with coupling.
c: Corresponds to layer 2 without coupling ($d_2 \to \infty$).
d: Corresponds to layer 1 without coupling ($d_2 \to \infty$).

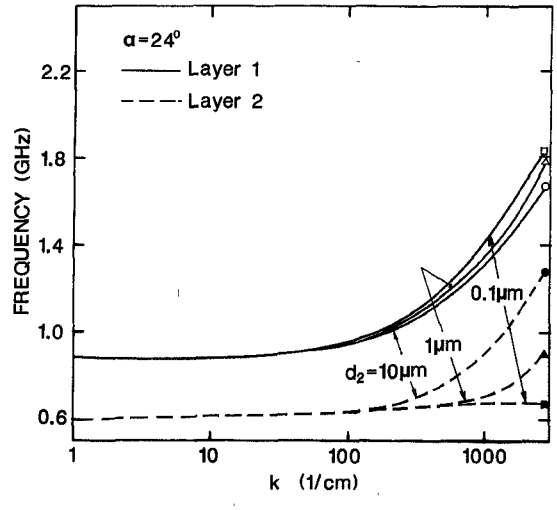

Fig. 6. Dispersion with $\theta_k = 0$, $H = 0$, and $\alpha = 24°$. The separation between the two magnetic layers is varied; i.e. d_2 is 0.1 μm, 1 μm, and 10 μm, respectively.

increases. The implication of having two time delays associated with two waves propagating in two layers is that one may input a wave in one layer with a certain time delay and detect the same wave in the other layer with different time delay. We note in Fig. 7 that there always exists a peak in time delay, corresponding to the layer with induced in-plane anisotropy. Also, the smaller the separation between the two layers, the stronger the coupling between the two layers. This results in a a higher peak in time delay.

Figs. 8 and 9 show the same features as Figs. 6 and 7. In this case we applied a field of 50 Oe in the $\langle 111 \rangle$ direction with the application of a magnetic field, resulting in a smaller value of α. Magnetostatic wave propagation with the greatest bandwidths may be assumed normal to both $\vec{M}_1$ and $\vec{M}_2$ in each layer so the wave in each layer contains wave components from the other layer arising from the coupling. Further increasing the bias magnetic field aligns $\vec{M}_1$ and $\vec{M}_2$ to-

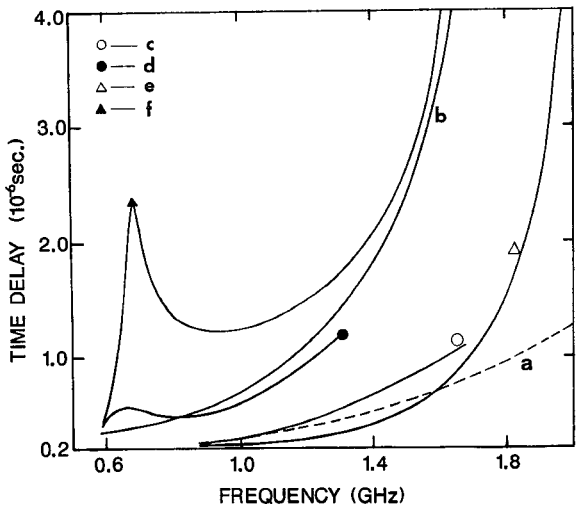

Fig. 7. Time delay versus frequency. $\theta_k = 0$, $H = 0$, and $\alpha = 24°$. The separation between the two magnetic layers is varied.

a: $d_2 \to \infty$. The branch corresponding to layer 1.
b: $d_2 \to \infty$. The branch corresponding to layer 2.
c: $d_2 = 10$ μm. The branch corresponding to layer 1.
d: $d_2 = 10$ μm. The branch corresponding to layer 2.
e: $d_2 = 1$ μm. The branch corresponding to layer 1.
f: $d_2 = 1$ μm. The branch corresponding to layer 2.

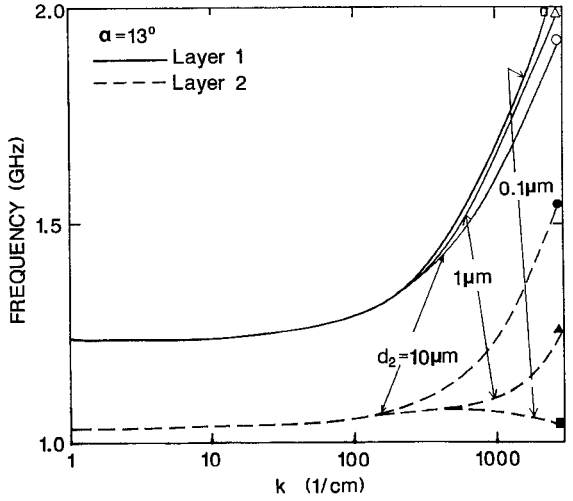

Fig. 8. Dispersion with $\theta_k = 0$, applied magnetic field $H = 50$ G, and $\alpha = 13°$. The separation between the two magnetic layers is varied as 0.1 μm, 1 μm, and 10 μm, respectively.

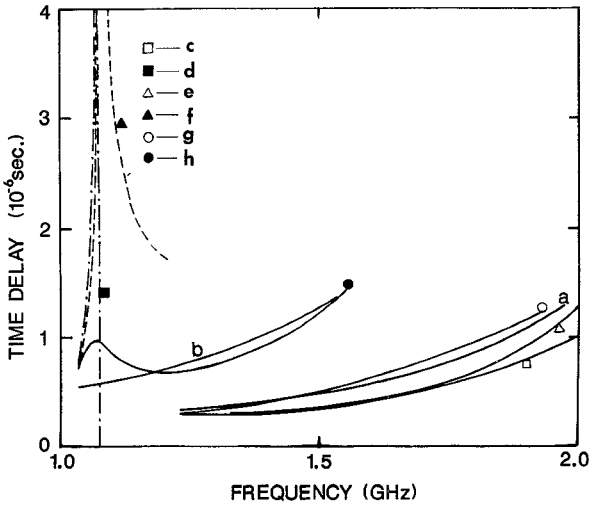

Fig. 9. Time delay versus frequency. $\theta_k = 0$, $H = 50$ G, and $\alpha = 13°$.

a: $d_2 \to \infty$. The branch corresponding to layer 1.
b: $d_2 \to \infty$. The branch corresponding to layer 2.
c: $d_2 = 0.1$ μm. The branch corresponding to layer 1.
d: $d_2 = 0.1$ μm. The branch corresponding to layer 2.
e: $d_2 = 1$ μm. The branch corresponding to layer 1.
f: $d_2 = 1$ μm. The branch corresponding to layer 2.
g: $d_2 = 10$ μm. The branch corresponding to layer 1.
h: $d_2 = 10$ μm. The branch corresponding to layer 2.

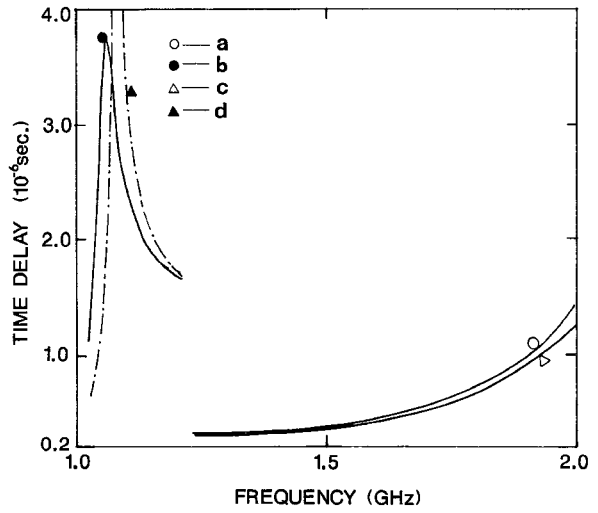

Fig. 10. Time delay versus frequency. $H = 50$ Oe. $\alpha = 13^0$ and $\theta_k = 0$. Curves *a* and *b* correspond to layers 1 and 2, respectively. For layer 2, $2K_u/M_2 = 80$ Oe. Curves *c* and *d* correspond to layers 1 and 2, respectively. For layer 2, $2K_u/M_2 = 50$ Oe.

gether and magnetostatic waves with desired property in both layers propagate in the same direction.

Anisotropy effects in wave propagation can be shown in Fig. 10. In this calculation, the cubic anisotropy constants for both magnetic layers are set to $2K_1/M = -82$ Oe, and the induced in-plane anisotropy constants are assumed to be different. For the layer with the higher $4\pi M$, we have $2K_u/M = 0$, while for the layer with lower $4\pi M$ we have $2K_u/M = 50$ and 80 Oe. As illustrated in Fig. 10, wave dispersions are directly affected by the values of H_u. For example, H_u affects the time delay, where the peak time delay is inversely proportional to H_u.

It is noted that all the above-mentioned propagations are in the positive directions. However, if the propagation directions are reversed, the corresponding dispersions are different from those with the positive directions [1], [5], [9], because this system is not symmetrical.

The double-layer YIG films with different orientations of magnetization potentially will find applications in a large number of microwave devices. For example, by applying the bias magnetic field along the easy axis ⟨111⟩, the angle α can be varied. This angle changes with the applied magnetic field. The weaker the applied field, the larger the angle α. Thus, if one can excite a magnetostatic wave in one layer, it may be possible to detect a magnetostatic wave of the greatest bandwidth with a different direction and velocity in

the other layer. By varying the magnitude of the applied magnetic field, the direction of wave propagation and time delay of interest can be changed over a certain range.

IV. Conclusions

We have calculated magnetostatic surface wave dispersion in double-layer structures in which the direction of the static magnetization in each layer is arbitrary. A general dispersion relation is obtained between frequency and the propagation constants k_y and k_z. Calculated results indicate that the separation between two magnetic layers and the induced in-plane anisotropy have very strong effects on the dispersion and time delay of the structure. Since the two magnetizations are not parallel, one can control the direction of wave propagation and the time delay by varying the applied magnetic field.

Acknowledgment

The authors wish to thank Dr. H. L. Glass, Dr. P. De Gasperis, and Dr. R. Marcelli for useful discussions pertaining to this work.

References

[1] T. Wolfram, "Magnetostatic surface waves in layered magnetic structures," *J. Appl. Phys.*, vol. 41, pp. 4748–4749, 1970.
[2] A. K. Ganguly and C. Vittoria, "Magnetostatic wave propagation in double layers of magnetically anisotropic slabs," *J. Appl. Phys.*, vol. 45, pp. 4665–4667, Oct. 1974.
[3] L. R. Adkins and H. L. Glass, "Magnetostatic volume wave propagation in multiple ferrite layers," *J. Appl. Phys.*, vol. 53, pp. 8928–8933, Dec. 1982.
[4] P. R. Emtage and M. R. Daniel, "Magnetostatic waves and spin waves in layered ferrite structures," *Phys. Rev. B*, vol. 29, pp. 212–220, Jan. 1984.
[5] V. I. Zubkov and V. A. Epanechnikov, "Surface magnetostatic waves in two-layer ferromagnetic films," *Sov. Tech. Phys. Lett.*, vol. 11, pp. 585–586, Dec. 1985.
[6] H. Pfeiffer, "Characteristics of magnetostatic surface waves for a system of two magnetic films," *Phys. Status Solidi*, vol. A18, pp. K53–K56, 1973.
[7] N. S. Chang and Y. Matsuo, "Numerical analysis of MSSW delay line using layered magnetic thin slabs," *Proc. IEEE*, vol. 66, pp. 1577–1578, Nov. 1978.
[8] H. Sasaki and N. Mikoshiba, "Directional coupling of magnetostatic surface waves in a layered structure of YIG films," *J. Appl. Phys.*, vol. 52, pp. 3546–3552, May 1981.
[9] P. Grünberg, "Magnetostatic spin-wave modes of a heterogeneous ferromagnetic double layer," *J. Appl. Phys.*, vol. 52, pp. 6824–6829, Nov. 1981.
[10] J. P. Parekh and K. W. Chang, "MSFVW dispersion control utilizing a layered YIG-film structure," *IEEE Trans. Magn.*, vol. MAG-18, pp. 1610–1612, Nov. 1982.
[11] R. E. Camley, T. S. Rahman, and D. L. Mills, "Magnetic excitations in layered medias: Spin waves and light-scattering spectrum," *Phys. Rev. B*, vol. 27, pp. 261–277, Jan. 1983.
[12] R. W. Damon and J. R. Eshbach, "Magnetostatic modes of a ferromagnet slab," *J. Phys. Chem. Solids*, vol. 19, pp. 308–320, 1961.
[13] K. Sun and C. Vittoria, H. L. Glass, P. De Gasperis, and R. Marcelli, "Ferromagnetic resonance of single crystal yttrium iron garnet/gadolinium gallium garnet/yttrium iron garnet layers," *J. Appl. Phys.*, vol. 67, no. 6, pp. 3088–3092, Mar. 1990.
[14] C. Vittoria and N. D. Wilsey, "Magnetostatic wave propagation losses in an anisotropic insulator," *J. Appl. Phys.*, vol. 45, pp. 414–420, Jan. 1974.

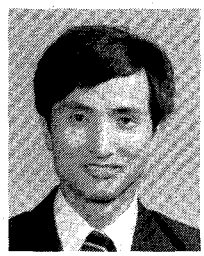

Kunquan Sun was born in Bengbu, China, on January 7, 1955. He received the B.S. and M.S. degrees from the University of Science and Technology of China, Hefei, People's Republic of China, in 1982 and 1984, respectively. He received the Ph.D. degree in electrical and computer engineering in 1990 from Northeastern University, Boston, MA.

He is now an Assistant Professor at Jackson State University, Jackson, MS. His present research interests include magnetostatic waves, microwave and millimeter circuits and devices, microstrip antennas, and the characterization and application of magnetic materials.

Carmine Vittoria (S'62–M'63–SM'83), photograph and biography not available at the time of publication.